Science of the Total Environment 625 (2018) 1615–1627

Contents lists available at ScienceDirect

Science of the Total Environment

journal homepage: www.elsevier.com/locate/scitotenv

Maintenance of photosynthesis by *Betula populifolia* in metal contaminated soils

Allyson B. Salisbury [a,*,1], Frank J. Gallagher [b], Joshua S. Caplan [c], Jason C. Grabosky [d]

[a] Department of Environmental Science, Rutgers, The State University of New Jersey, 14 College Farm Road, New Brunswick, NJ 08901, USA
[b] Department of Landscape Architecture, Rutgers, The State University of New Jersey, 93 Lipman Drive, New Brunswick, NJ 08901, USA
[c] Department of Landscape Architecture and Horticulture, Temple University, 580 Meetinghouse Road, Ambler, PA 19002, USA
[d] Department of Ecology, Evolution, and Natural Resources, Rutgers, The State University of New Jersey, 14 College Farm Road, New Brunswick, NJ 08901, USA

HIGHLIGHTS

- *B populifolia* photosynthetic parameters were similar in soils with low and high metal loads.
- After a heat wave, water use efficiency was significantly higher for trees in soils with low metal loads.
- Other parameters differed by metal load only in particular months.

GRAPHICAL ABSTRACT

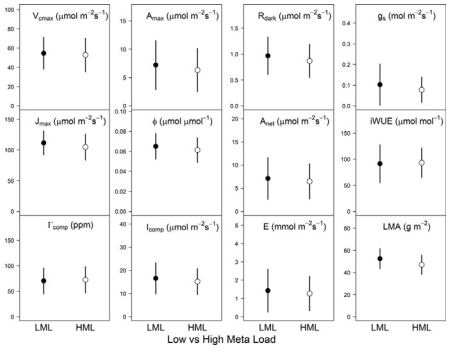

ARTICLE INFO

Article history:
Received 10 October 2017
Received in revised form 22 December 2017
Accepted 23 December 2017
Available online xxxx

Editor: Charlotte Poschenrieder

Keywords:
Light response curve
Assimilation-intercellular CO_2 (A-C_i) curve
Heavy metals

ABSTRACT

Improving our understanding of plant responses to elevated trace metal concentrations under field conditions will enhance restoration and urban greening practices in settings with contaminated soils. This study examined the effects of trace metal pollution on the leaf gas exchange rates of mature, field-grown *Betula populifolia* Marsh. (gray birch) trees, additionally assessing whether elevated temperature and drought compounded the effects of trace metal contamination. The study compared *B. populifolia* growing in areas of comparatively high and low trace metal loads (HML and LML, respectively) within a former rail yard at Liberty State Park in Jersey City, New Jersey, USA. Gas exchange parameters were determined monthly from May through September in 2014 and 2015 using a portable photosynthesis system. The effects of drought and high temperature were assessed during a short heat wave in July 2015 and via a manipulative experiment, respectively. During a few of the measurement months, some parameters differed significantly between the LML and HML groups. However, when considered over the entire study period, no significant differences in biophysical parameters were observed

Abbreviations: A_{max}, Maximum net photosynthetic assimilation rate; A_{net}, Net photosynthetic assimilation rate; C_i/C_a, Ratio of intercellular to ambient CO_2 concentration; E, Transpiration rate; g_s, Stomatal conductance of water vapor rate; HML, High metal load; I_{comp}, Light compensation point; iWUE, Intrinsic water use efficiency; J_{max}, Maximum electron transport rate; LML, Low metal load; LSP, Liberty State Park; R_{dark}, Dark respiration rate; TML, Total Metal Load Index; V_{cmax}, Maximum Rubisco carboxylation rate; Γ_{comp}, CO_2 compensation point; φ, Quantum yield.

* Corresponding author.
E-mail addresses: allyson.salisbury@rutgers.edu (A.B. Salisbury), gallagher@sebs.rutgers.edu (F.J. Gallagher), jcaplan@temple.edu (J.S. Caplan), grabosky@sebs.rutgers.edu (J.C. Grabosky).
[1] Present address: Department of Biology, Rutgers-Newark, The State University of New Jersey, 195 University Avenue, Newark, NJ 07102, USA..

https://doi.org/10.1016/j.scitotenv.2017.12.279
0048-9697/© 2017 Published by Elsevier B.V.

Phytostabilization
Stomatal conductance
Dark respiration

between groups. The photosynthetic capacity of *B. populifolia* thus appears to be fairly robust across this site's steep gradient of trace metal contamination. Nonetheless, leaf mass per unit area was significantly lower in the HML group, indicating that metal loads affected resource allocation within trees. Also, immediately following the heat wave in 2015, intrinsic water use efficiency declined significantly in the HML group, suggesting that extreme climatic conditions can have a disproportionate effect on the physiological performance of plants growing in metal contaminated soils.

© 2017 Published by Elsevier B.V.

1. Introduction

Soil contamination by trace metals (also referred to as trace elements or heavy metals) poses a significant threat to human and ecological health, as industrial activities in both rural and urban areas have yielded high trace metal concentrations in soils globally (Ajmone-Marsan and Biasioli, 2010; Larson, 2014; Panagos et al., 2013). Human exposure risk will likely intensify as urban populations expand, especially due to high rates of immigration to cities (United Nations, 2015). Plant communities can play an important role in managing soil trace metal contamination; plants limit soil erosion, maintain aerobic belowground conditions, and generate organic compounds capable of binding trace metals (Robinson et al., 2009). Revegetation can therefore be a cost-effective restoration strategy for degraded sites (Prach and Pysek, 2001; Sebelikova et al., 2016). However, maintaining plant communities at sites that are contaminated or otherwise highly disturbed can be challenging due to the abiotic stresses imposed by soil conditions (Pavao-Zuckerman, 2008). A greater understanding of plant physiological responses to growth in trace metal contaminated soils, especially in species that appear to be well adapted to such conditions, would provide insight into the extent to which organismal and community-level processes can be maintained in the face of trace metal contamination.

Prior studies have identified an array of stress responses to trace metal exposure in plants. For example, trace metals can reduce chlorophyll production, interact with enzymes, change the function of chloroplast membranes, inhibit photosystem I and photosystem II, and impair stomatal function (Mysliwa-Kurdziel et al., 2004). Additionally, trace metals are known to affect water transport through roots (Maggio and Joly, 1995), decrease the diameter and number of xylem vessels (Robb et al., 1980), induce stomatal closure (Moustakas et al., 1997), and trigger a stress response similar to that from water deficiency (de Silva et al., 2012). However, most prior studies have occurred in laboratory or greenhouse settings, such that the array of biotic and abiotic interactions that plants experience in the field are not well represented in these experiments. The ecophysiological responses and tradeoffs that take place in mature individuals from longer lived species (e.g., trees) are particularly poorly understood. Moreover, given that photosynthetic responses to trace metal stress can vary among genotypes within a single species (Gaudet et al., 2011), it could be especially valuable to determine how mature plants from genotypes that have proven to be tolerant of high soil trace metal concentrations perform in a field context.

Extreme weather conditions may have particularly large effects on plants growing in metal contaminated soils, though this is not well studied under field conditions. We know, for example, that trace metal exposure can change xylem structure, increase stomatal resistance, reduce leaf size, and induce abscission; these responses may also promote water conservation and mitigate the effects of drought (Poschenrieder and Barcelo, 2004). However, the extent to which restricting water use induces tradeoffs in carbon assimilation is difficult to predict; such effects may be minimal in well-adapted species but highly inhibiting otherwise (Santala and Ryser, 2009; de Silva et al., 2012). Moreover, the increasing frequency of drought and the rising temperatures associated with climate change may exacerbate physiological stresses induced by exposure to trace metals (Romero Lankao et al., 2014), especially given that water availability also tends to be limited in degraded soils (Pavao-Zuckerman, 2008). Changes in temperature and precipitation regimes may further alter soil pH and redox conditions, consequently affecting trace metal speciation and mobility (Al-Tabbaa et al., 2007). In the context of managing plant assemblages at contaminated sites, it would be useful to identify the thresholds at which the combined effects of extreme weather events and trace metal exposure exceed the limits of well-adapted species to acclimate to and/or tolerate their conditions. Understanding the interacting effects of extreme weather and trace metal contamination on plant performance is therefore necessary to ensure the long term stability of vegetation at contaminated sites.

Trace metal contamination of soil can impair ecosystem functions. Understanding the ecosystem-scale response to stress from soil pollution is highly relevant in the context of restoration (Hooper et al., 2016) and urban greening projects (Doick et al., 2009), as these are likely to involve degraded and/or polluted soils. However, it is difficult to assess or predict the impact of high soil metal loads on ecosystem functions such as primary productivity (Rohr et al., 2016). Instead, most research has studied contaminant effects at the organismal scale (Martin et al., 2014). Extrapolating these effects into higher levels of biological organization is challenging because of compounding variables such as climate, intra- and interspecific competition, and feedback loops (De Laender et al., 2008).

One approach to improving our mechanistic understanding of trace metal impacts on ecosystem properties such as primary productivity is to determine how trace metals affect leaf-level physiology. Information on gas exchange can further refine our understanding of plant stress responses to trace metal pollution (Rachmilevitch et al., 2006). Photosynthetic gas exchange parameters can also be utilized in approaches such as forest dynamics models (e.g. Medvigy et al., 2009), predictive system models (e.g. Forbes and Calow, 2013), or dynamic energy budget models (e.g. Martin et al., 2013) to scale trace metal effects from the leaf level to that of the forest stand.

We evaluated the ecophysiological performance of a tree species that is widespread in trace metal contaminated sites, *Betula populifolia* Marsh., under field conditions spanning modestly to highly contaminated. Members of the *Betula* genus are commonly found in degraded and/or trace metal contaminated soils (e.g., Bleeker et al., 2002; Borgegard and Rydin, 1989; Frouz et al., 2008; Murray et al., 2000) and have been used in brownfield greening projects (Doick et al., 2009; French et al., 2006). We specifically set out to answer the following questions:

1) Does gas exchange differ at the two levels of soil contamination in mature, self-seeded trees of *B. populifolia* and how consistent is the effect through the growing season?
2) Do trees growing in soils with higher concentrations of soil trace metals experience greater reductions or tradeoffs in gas exchange under high heat or drought conditions?

Based prior work at our study site (Dahle et al., 2014; Gallagher et al., 2008a; Radwanski et al., 2017; Renninger et al., 2013), we hypothesized that trees growing in soils with the highest concentrations of trace metals would exhibit reduced or impaired photosynthesis and transpiration related processes. We further hypothesized that high heat and water stress would accentuate the effect of trace metal exposure on gas exchange parameters in *B. populifolia*.

2. Methods

2.1. Study site

This study took place in an undeveloped, interior portion of Liberty State Park (LSP) in Jersey City, New Jersey, USA (Fig. 1; 40° 42′ 16″ N, 74° 03′ 17″ W). LSP is built on a filled tidal marsh that was the site of a rail yard and industrial area for more than a century before they were abandoned in 1967. The soil consists entirely of anthropogenic fill and has several layers of unique debris horizons; it is classified as a sandy-skeletal, over loamy, mixed, mesic Oxyaquic Udorthent with 0 to 3% slopes (Soil Survey Staff, 2010). Concentrations of numerous trace metal(loids)s exceed background levels, but arsenic (As), chromium (Cr), copper (Cu), lead (Pb), and zinc (Zn) are sufficiently concentrated in portions of the site to additionally exceed residential or ecological screening criteria (Gallagher et al., 2008b). An index of total metal load (TML) spanning the range of trace metals present at 22 plots at the site was previously developed from concentrations of As, Cr, Cu, Pb, and Zn; values range from 0 (very low concentrations) to 5 (very high concentrations) (Gallagher et al., 2008b). A lack of human intervention in the interior portion of LSP allowed a spontaneous plant community to establish shortly after abandonment, and community dynamics have played out in the decades since then to the extent that much of the site is now dominated by woody plants (Gallagher et al., 2011). LSP is otherwise a typical post-industrial site with a history of neglect but with promise for adaptive reuse as a natural area.

2.2. Plot selection

To compare plant performance under higher vs. lower concentrations of trace metals, we took advantage of spatial variation in trace metal contamination across the site. We used four hardwood plots (1000 m^2) for this study; two had soils below the total metal load (TML) threshold of 3 (plots L1 and L2; Gallagher et al., 2008a, b) and two had soils above the threshold (plots H2 and H3; Table 1). All four study plots were located in early successional hardwood stands that were predominantly composed of *B. populifolia*; the primary co-dominant trees were *Populus deltoides* W. Bartram ex Marshall and *Populus tremuloides* Michx. Soils underlying the four plots were similar in texture, though phosphorus and pH differed significantly among plots (Table 1).

2.3. Weather data

Hourly and daily data on temperature, precipitation, relative humidity, and solar radiation for the study period were collected at a weather station operated by New Jersey Mesonet (station 3411; New Jersey Weather and Climate Network, 2016), located within 1200 m of all study plots. Reference evapotranspiration (ETo) was used as a metric of atmospheric demand for water and calculated using the Penman-Monteith equation following the procedure outlined by the Food and Agricultural Organization (FAO; Allen et al., 1998). As recommended by the FAO, the hypothetical reference crop was presumed to have a height of 0.12 m, a fixed surface resistance of 70 s m^{-1}, and an albedo of 0.23 (Allen et al., 1998).

2.4. Gas exchange measurement

Measurements of leaf gas exchange were made on 20 trees each month from May through September in both 2014 and 2015. Within each of the four plots, five mature *B. populifolia* trees were selected based on their diameter at breast height (DBH) to ensure individuals were selected from the 2nd, 3rd, and 4th quartiles of the DBH distribution

Fig. 1. Study area in the interior of Liberty State Park. Point labels that include *H* indicate plots with high trace metal concentrations while labels that include *L* indicate plots with comparatively low concentrations.

Table 1
Mean values (±1 SD) for soil properties at the four study plots. Within each row, differences between plots at the 95% confidence level are indicated by different letters, as determined from Tukey HSD tests. *TML*, total metal load; *TKN*, total Kjeldahl nitrogen; *TN*, total nitrogen; *TC*, total carbon. *Previous label* indicates plot names used in other publications. † data were natural log transformed prior to analysis.

Soil property	Plot L1	Plot L2	Plot H2	Plot H3
Previous label	TP-0041	TP-0048	TP-1416	TP-0025
TML	0.85	1.56	3.56	4.31
As (μg g^{-1})	13.3 ± 3.7	10.7 ± 5.9	42.8 ± 9	270 ± 184
Cr (μg g^{-1})	9.7 ± 4.4	16.7 ± 20.0	209 ± 59.4	40.4 ± 26.1
Cu (μg g^{-1})	68.4 ± 23.7	76.4 ± 18.0	129 ± 11.2	1527 ± 219
Pb (μg g^{-1})	86.1 ± 27.6	196 ± 83.8	552 ± 73.6	4640 ± 1210
Zn (μg g^{-1})	198 ± 103	24.9 ± 12.3	157 ± 51.5	1586 ± 1358
Texture	Loamy sand	Loamy sand	Loamy sand	Sand/Loamy sand
pH	5.5^{b} ± 0.3	6.1^{a} ± 0.3	5.4^{b} ± 0.1	5.4^{b} ± 0.3
P (μg g^{-1})†	79.9^{a} ± 68.9	6.7^{b} ± 1.2	82.0^{a} ± 16.7	5.8^{b} ± 2.7
K (μg g^{-1})	57.9^{a} ± 13.7	48.5^{a} ± 9.7	76.9^{a} ± 8.9	61.9^{a} ± 25.5
Mg (μg g^{-1})†	93.8^{a} ± 37.4	77.7^{a} ± 50.3	101.6^{a} ± 21.7	96.5^{a} ± 65.7
Ca (μg g^{-1})†	467^{a} ± 417	394^{a} ± 305	305^{a} ± 142	428^{a} ± 299
TKN (%)†	0.25^{a} ± 0.1	0.23^{a} ± 0.06	0.3^{a} ± 0.03	0.18^{a} ± 0.1
TN (%)	0.31^{a} ± 0.27	0.43^{a} ± 0.16	0.55^{a} ± 0.33	0.37^{a} ± 0.12
TC (%)	11.7^{b} ± 8.3	22.0^{a} ± 2.0	24.6^{a} ± 7.8	18.4^{a} ± 5.0
Nutrient samples	4	3	4	4

previously determined for the population (Dahle et al., 2014). In most cases, the same trees were measured each month. However, due to storm damage from the previous year, several trees deteriorated to the extent that all accessible branches had died; in subsequent months measurements were made from adjacent trees. All gas exchange measurements were made on excised branches collected approximately 5 m above ground level; cut surfaces were immediately placed in water and recut while submerged to prevent xylem cavitation (Joesting et al., 2009; Kubiske and Pregitzer, 1996; Reich et al., 1995).

To quantify leaf photosynthetic traits, two sets of gas exchange measurements were made using an LI-6400XT portable gas exchange system (LI-COR Biosciences, Lincoln, USA). These were typically made between the hours of 8:00 and 13:00 using the most apical and second-most apical expanded and undamaged leaves from each excised branch. Photosynthetic light-response curves (i.e., light curves) were generated using the following photosynthetic photon flux density (PPFD) sequence: 2000, 1500, 1000, 500, 200, 100, 50, 20, 0 μmol m^{-2} s^{-1}. During these measurements reference CO_2 was maintained at 400 μmol mol^{-1}. Responses of photosynthesis (specifically net carbon assimilation, or A_{net}) to changing intercellular CO_2 concentrations (i.e., A-C_i curves) were evaluated using a second set of measurements maintained at constant PPFD (1500 μmol m^{-2} s^{-1}); cuvette CO_2 concentrations were varied through the following sequence: 400, 300, 200, 100, 50, 400, 400, 600, 700, 800, 900, 1000, 1500 μmol mol^{-1}. For both sets of measurements, relative humidity in the sample chamber was maintained between 60 and 80% and block temperature was set to 25 °C.

Light curves were fit with nonlinear least squares regression using the non-rectangular parabolic equation developed by Prioul and Chartier (1977). This yielded the maximum net assimilation rate (A_{max}), quantum efficiency (φ), and dark respiration rate (R_{dark}). The light compensation point (I_{comp}) was calculated from the parameterized equation by solving the fitted model for $A_{net} = 0$. A-C_i curves were fit with the Farquhar-von Caemmerer-Berry model of C_3 photosynthesis (Farquhar et al., 1980), which yielded the maximum carboxylation rate (V_{cmax}) and maximum electron transport rate (J_{max}). Curves were fit using the *plantecophys* package in the R computing environment (Duursma, 2015; R Development Core Team, 2016). One challenge in fitting A-C_i curves is identifying the level of intercellular CO_2 (C_i) where one limitation transitions to another (i.e., the C_i transition point), especially given that, at some concentrations, both Rubisco and RuBP regeneration can be co-limiting (Sharkey et al., 2007). The algorithm used by *plantecophys* obviates the need to manually determine the C_i transition point for each curve. To compare enzymatically-mediated rates at equivalent temperatures, V_{cmax} and J_{max} were normalized to 25 °C using the constants provided in Appendix B. Otherwise, the default settings in *plantecophys* were used for fitting. The CO_2 compensation point (Γ_{comp}) was calculated by solving the fitted model for $A_{net} = 0$.

Intrinsic water use efficiency (iWUE, also called potential water-use efficiency or physiological water-use efficiency) was calculated as iWUE $= A_{net}/g_s$, where A_{net} is the net photosynthetic assimilation rate (μmol CO_2 m^{-2} s^{-1}) and g_s is stomatal conductance to water vapor (mol H_2O m^{-2} s^{-1}). A_{net} and g_s were determined from light curve measurements made at 400 ppm CO_2 and 1500 μmol PAR m^{-2} s^{-1}.

2.5. Temperature and drought response

To determine if soil metal loads compounded the effects of high temperature, an additional set of A-C_i curves was collected on 25–26 July 2014. Five trees from a high metal plot (H3) and five trees from a low metal plot (L1) were used in the temperature study; none of these trees were used in the primary study. Temperature was controlled by setting the LI-6400XT block temperature to 25, 30, and 35 °C, though realized leaf temperatures varied from 25.4 to 34.4 °C. A different branch was excised for each temperature level and acclimated to cuvette conditions until readings stabilized. All other settings for the A-C_i curves were the same as those described in Section 2.4.

While June 2015 was wetter than average, several days of high temperatures and no rainfall occurred the following month that strongly affected photosynthesis parameters. During this "heat wave" (19–21 July 2015), daily maximum temperatures were 33 to 35.5 °C and daily reference evapotranspiration (ETo) ranged from 1.3 to 4.7 mm day^{-1} (Fig. 2). A total of 1.8 cm of rain had fallen in the preceding two weeks, leading to substantial soil water deficits. Preliminary measurements made on 21 July indicated that photosynthetic rates were substantially lower than normal. Consequently, additional survey measurements were made on 22-23 July (daily maximum temperature = 30 °C; ETo = 8.7 and 8.3 mm day^{-1}) in order to capture net photosynthetic assimilation (A_{net}), transpiration (E), stomatal conductance (g_s), and intrinsic water use efficiency (iWUE) from all of the study trees while the effects of the heat wave persisted. Measurements were made on leaves of excised branches at 400 μmol CO_2 mol^{-1} air and 1500 μmol photons m^{-2} s^{-1}. A leaf was placed in the sample chamber, then, once CO_2 and H_2O concentrations stabilized, a single measurement was made.

2.6. Leaf mass per area

Leaf mass per unit area (LMA) was measured as a metric of trees' investment in leaf tissue. Data were collected from all leaves used for gas exchange measurements in 2015. Leaves were imaged using an Expression 10000XL flatbed scanner (Epson America, Long Beach, USA) and their areas were measured using ImageJ software (Ferreira and Rasband, 2012). Leaves were oven dried at 60 °C for at least 72 h then cooled in a desiccator and weighed. LMA was calculated by dividing the leaf dry weight (g) by the leaf area (m^2).

2.7. Statistical analysis

Mixed effects linear models were used to evaluate the effects of metal load and measurement period on each photosynthesis parameter. Metal load (a discrete variable with two levels), month-year (a discrete variable with 10 levels), and their interaction were treated as fixed effects while tree and plot were treated as random effects. J_{max}, Γ_{comp}, I_{comp}, E, and g_s were natural log transformed to achieve residual normality. The significance of fixed effects was determined using *F*-tests based on Type III sums of squares. When parameters had significant interaction effects, *post hoc* comparisons of metal load levels within each month-year period were further analyzed using least-squares means (i.e., population marginal means; Searle et al., 1980). This entailed determining if the estimated difference between means at each metal level differed from zero; Tukey-adjusted 95% confidence intervals

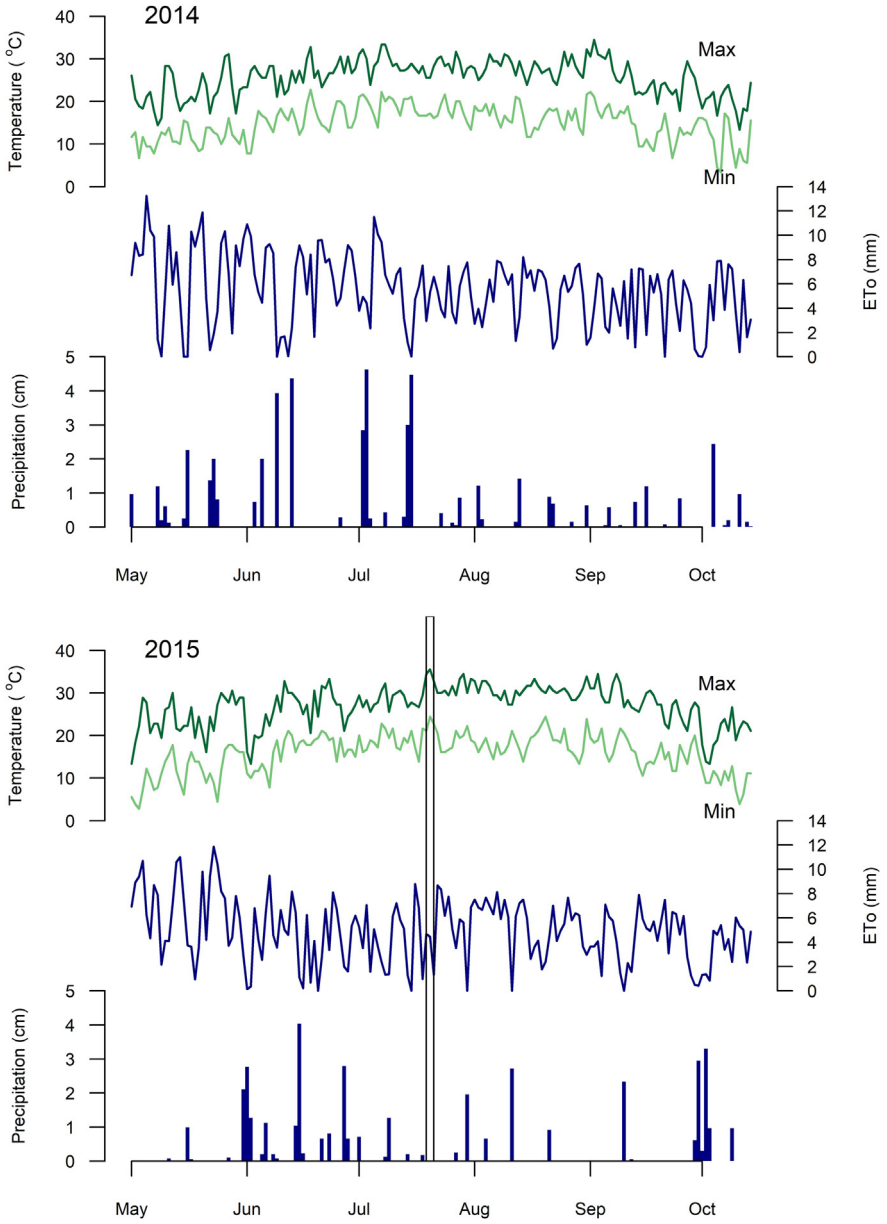

Fig. 2. Daily maximum and minimum temperatures, reference evapotranspiration (ETo), and precipitation in Jersey City, New Jersey, USA from May to October 2014 and 2015. The heat wave in July 2015 is indicated by black box. Data from NJ Mesonet weather station 3411 (New Jersey Weather and Climate Network, 2016).

were used for this determination. In some months later in the growing season, photosynthesis rates were too low to obtain accurate parameters from the light or A-Ci curves, leading to gaps in the dataset. The least-squares means approach is able to compensate for this lack of balance (Lenth, 2016). The concentration of plant available phosphorus and soil pH differed significantly among study plots (Table 1), potentially confounding metal load effects. However, a companion study indicated that soil metals had significantly more influence than nutrient concentrations or pH on the spatial distribution of trees at the site (Menese-Florian, et al., unpublished). Moreover, an additional random effect for phosphorus level that was included in initial models did not improve model performance; it was excluded from final models. Finally, in most regression models tree identity accounted for greater variation in the response than plot (Table 2), further suggesting that plot level variation did not substantially influence model fit.

The effects of leaf temperature on A-C_i curve parameters, as determined by the temperature response study, were evaluated using linear regression. Terms included leaf temperature (a continuous variable), metal load level (LML or HML), and their interaction. Most response variables were untransformed, but g_s and E were natural log transformed to normalize residuals. Soil properties were compared among the four plots using a one-way ANOVA and Tukey HSD tests. Phosphorus, magnesium, calcium, and total Kjeldahl nitrogen were natural log transformed prior to analysis. All data analyses were performed using R version 3.3.1 (R Development Core Team, 2016), including the function libraries *car* (Fox and Weisberg, 2011), *lattice* (Sarkar, 2008), *lme4* (Bates et al., 2015), *lsmeans* (Lenth, 2016) and *agricolae* (de Mendiburu, 2016).

3. Results

3.1. Primary responses to trace metals

Six of the eleven photosynthesis parameters we measured, as well as LMA, differed significantly between metal load levels during at least one

Table 2
Mixed model results for the effects of metal load, month-year, and their interaction on gas exchange parameters and leaf mass per area. Results with a *P*-value <0.05 are bolded. Also shown are the standard deviations of random effects for the full model. Group means from the full model are provided in **Appendix C**.

	Fixed effects			Random effects		
	Metal load	Month-Year	Interaction	Tree	Plot	Residual
Parameter	*P*-value			Std. Dev.		
V_{cmax}	0.739	<**0.001**	0.080	3.594	0.000	12.859
J_{max}	0.417	0.786	**0.037**	0.000	0.044	0.198
Γ_{comp}	0.252	<**0.001**	0.070	0.057	0.000	0.203
A_{max}	0.288	<**0.001**	0.511	1.059	0.000	3.309
φ	0.485	<**0.001**	**0.041**	0.000	0.004	0.011
I_{comp}	0.266	0.219	0.084	0.000	0.000	0.398
R_{dark}	0.341	<**0.001**	0.115	0.086	0.047	0.292
A_{net}	0.510	<**0.001**	0.290	1.103	0.116	3.288
E	0.985	<**0.001**	0.660	0.231	0.000	0.650
g_s	0.430	<**0.001**	0.504	0.282	0.000	0.697
iWUE	0.941	<**0.001**	**0.054**	10.692	1.522	26.817
LMA	**0.008**	0.105	0.075	3.025	0.000	8.195

measurement period. In July 2014, J_{max}, φ, and R_{dark} were significantly higher for low metal load trees compared to high metal load trees (Table 3). Additionally, in June 2015, low metal load trees' Γ_{comp} and R_{dark} were higher than their high metal load counterparts, as was their iWUE the following month. Finally, I_{comp} was significantly greater in high metal load trees in September 2014. However, parameter means did not differ by metal load when data from all months were pooled (Fig. 3). Nonetheless, leaf mass per area (LMA) did differ by metal load, with mean LMA in low metal load trees significantly greater than that in high metal load trees (Table 2, Fig. 3).

Non-significant trends in many gas exchange parameters suggested that high metal loads induced modestly greater levels of physiological stress in *B. populifolia* trees than did low metal loads (Fig. 3). Specifically, sample means of V_{cmax}, J_{max}, maximum net assimilation (A_{max}), light compensation point (I_{comp}), quantum efficiency (φ), dark respiration rate (R_{dark}), net assimilation (A_{net}), transpiration (E), and stomatal conductance (g_s) were all lower in trees that had greater exposure to trace metals, while CO_2 compensation point (Γ_{comp}) and intrinsic water use efficiency (iWUE) were higher. Again, while the direction of differences in sample means was consistent with our hypotheses, there was insufficient statistical evidence to conclude definitively that these patterns were nonrandom.

3.2. Temperature and drought response

Immediately after the heat wave in July 2015, all plots exhibited lower A_{net} and g_s but higher iWUE (Fig. 4) as well as diminished V_{cmax}, A_{max}, φ, and R_{dark} (data not shown) compared to the month prior and the following two months. Moreover, in the days following the heat wave iWUE for the high metal load group was significantly lower than it was for the low metal load group (Table 3, Fig. 4). In the measurement periods after the heat wave (i.e., August and September 2015), all rates returned to levels similar to those observed in the previous year.

Analysis of the relationship between g_s and the ratio of intercellular to ambient CO_2 (C_i/C_a) indicated that the depression of photosynthetic rates observed during the July 2015 heat wave may have been due, at least in part, to non-stomatal limitations. For most of the study months, g_s followed the expected exponential rise with increasing C_i/C_a, such that higher C_i/C_a was associated with greater g_s; this relationship was not affected by metal load (Fig. D.1). However, C_i/C_a increased substantially at very low g_s in July and August 2015 despite some measurements exhibiting a very sharp decline in C_i/C_a with decreasing g_s. These observations occurred in all four study plots and are characteristic of non-stomatal processes (e.g., damage to photosynthetic apparatus from prolonged water deficit) limiting photosynthesis at these times (Brodribb, 1996).

Varying leaf temperature from 25 to 35 °C altered V_{cmax}, J_{max}, Γ_{comp}, and g_s, though no interaction effects with metal load were observed (Fig. 5). Specifically, positive relationships were observed for V_{cmax}, J_{max}, and Γ_{comp}, while the other significant parameters decreased with increasing temperature. The one parameter for which a non-significant trend suggested that high metal loads may alter values was J_{max}; values from high metal load trees were consistently lower than those from the low metal load trees spanning 28–31 °C (Fig. 5). Transpiration was not significantly affected by leaf temperature.

4. Discussion

4.1. Primary responses to trace metals

Some photosynthesis parameters exhibited a response to metal load during particular months of the year, lending partial support to our initial hypothesis that growth in soils with high trace metal concentrations would impair gas exchange. These transient responses to soil metal load

Table 3
Contrast estimates (±1 SE) for gas exchange parameters, i.e., the difference between LML and HML as determined by least-squares means, in each measurement month. Positive values indicate that the parameter was greater under LML than under HML; contrasts that differ significantly from zero are shown in bold. Empty cells indicate that there were insufficient data to calculate a contrast for that month. Parameters with no significant contrasts were omitted from the table. °P<0.1, * P<0.05, ** P<0.01. † indicates data were log transformed.

Month-Year	V_{cmax}	J_{max}†	Γ_{comp}†	A_{max}	φ	I_{comp}	R_{dark}	A_{net}	iWUE	LMA
May 2014	−9.0	−0.24°	0.04	0.4	−0.009	0.22	0.05	0.5	−5.0	
	±6.0	±0.12	±0.10	±1.6	±0.006	±0.18	±0.14	±1.6	±12.9	
Jun 2014	−2.4	0.02	−0.01	1.5	−0.001	−0.18	−0.11	2.5	−19.3	
	±6.1	±0.13	±0.10	±1.6	±0.006	±0.18	±0.15	±1.6	±13.3	
Jul 2014	10.8°	**0.27***	−0.03	1.1	**0.014***	0.32°	**0.30***	1.1	−19.2	
	±6.0	**±0.11**	±0.10	±1.6	**±0.006**	±0.18	**±0.14**	±1.6	±12.9	
Aug 2014	−8.8	0.19	0.07	−2.5	0.009	0.12	0.18	−2.83°	−8.8	
	±6.0	±0.15	±0.10	±1.6	±0.006	±0.18	±0.15	±1.6	±12.9	
Sep 2014	3.8		−0.15	1.0	0.009	**−0.35***	−0.17	1.0	22.0°	
	±6.0		±0.10	±1.6	±0.006	**±0.18**	±0.14	±1.6	±12.9	
May 2015	10.3	0.11	−0.02	2.7°	0.005	−0.07	0.05	2.3	−11.7	−0.09
	±6.9	±0.13	±0.11	±1.6	±0.006	±0.18	±0.15	±1.6	±12.9	±3.0
Jun 2015	−8.1	0.10	**0.27****	1.9	0.004	0.37°	**0.36***	2.0	−5.7	**10.0****
	±6.1	±0.12	**±0.10**	±1.6	±0.006	±0.19	**±0.15**	±1.6	±12.9	**±3.0**
Jul 2015	−4.0		0.24°	0.3	0.004	−0.04	0.04	−0.2	**36.3***	**7.7***
	±8.9		±0.14	±2.2	±0.008	±0.25	±0.2	±1.3	**±15.4**	±3.1
Aug 2015				0.3	−0.003	0.26	0.14	0.04	−6.1	3.0
				±1.8	±0.007	±0.20	±0.16	±1.6	±12.9	±3.0
Sep 2015								−1.1	12.5	5.6°
								±1.6	±12.9	±3.0

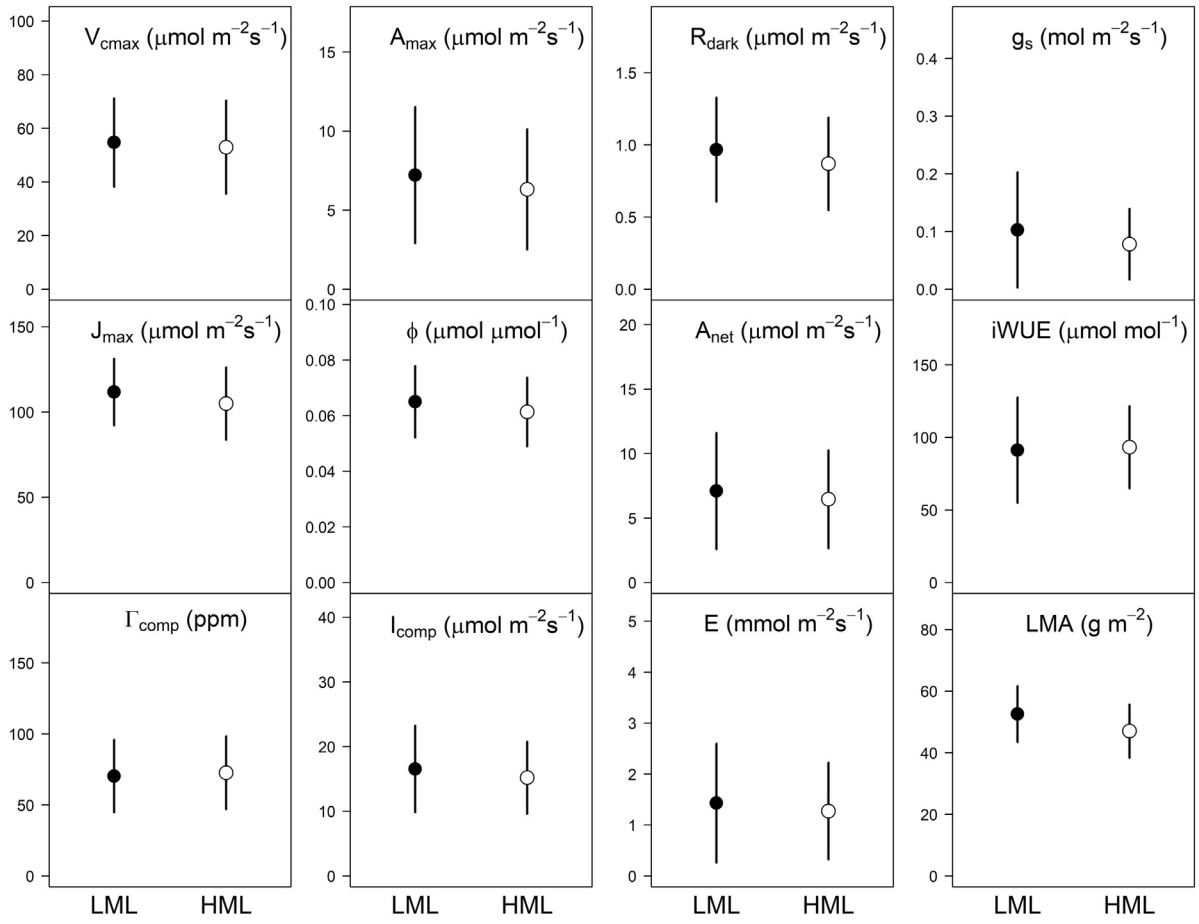

Fig. 3. Mean (±1 SD) gas exchange parameter values averaged over the entire study period, grouped by metal load. *LML*, low metal load; *HML*, high metal load.

may be attributable to changes in trace metal concentrations in leaves; the concentration of Zn in *B. populifolia* leaves was previously observed to vary over the course of the growing season at the site, with the peak concentration during the measurement year occurring in June (Gallagher et al., 2008a). While the effects of high metal loads that this study identified may be transient, they could have substantial effects on whole-tree growth rates if they occur during a critical part of the growing season (Boone et al., 2004).

That trees produced leaves with lower LMA (i.e., were thinner or lower density) when they grew in soils with high metal loads may indicate that these trees preferentially allocated photosynthate to organs other than leaves (notably roots; Gallagher et al., 2015) or that they had prohibitively high maintenance requirements. Consistent with this finding, other studies have found LMA to decrease with increasing soil metal concentrations (Di Baccio et al., 2009; Renninger et al., 2013) though others found no effect (André et al., 2006; Shi and Cai, 2009) or species-specific effects (Hermle et al., 2006). Also, *B. populifolia* LMA values ranged from 74 to 95 g m^{-2} when grown in uncontaminated soils (Chen et al., 2014; Wayne and Bazzaz, 1993); this exceeds the vast majority of our measurements (which ranged from

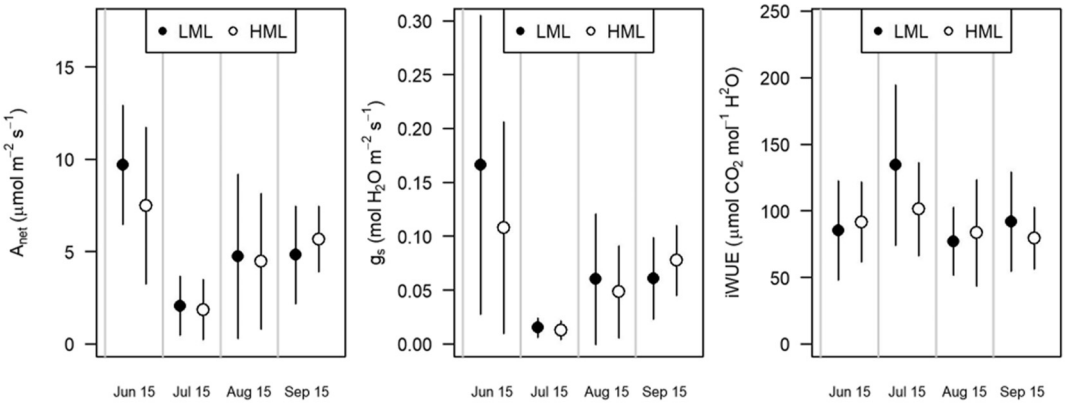

Fig. 4. Mean (±1 SD) values of gas exchange parameters before (June), immediately after (July) and well after (August and September) the 2015 heat wave.

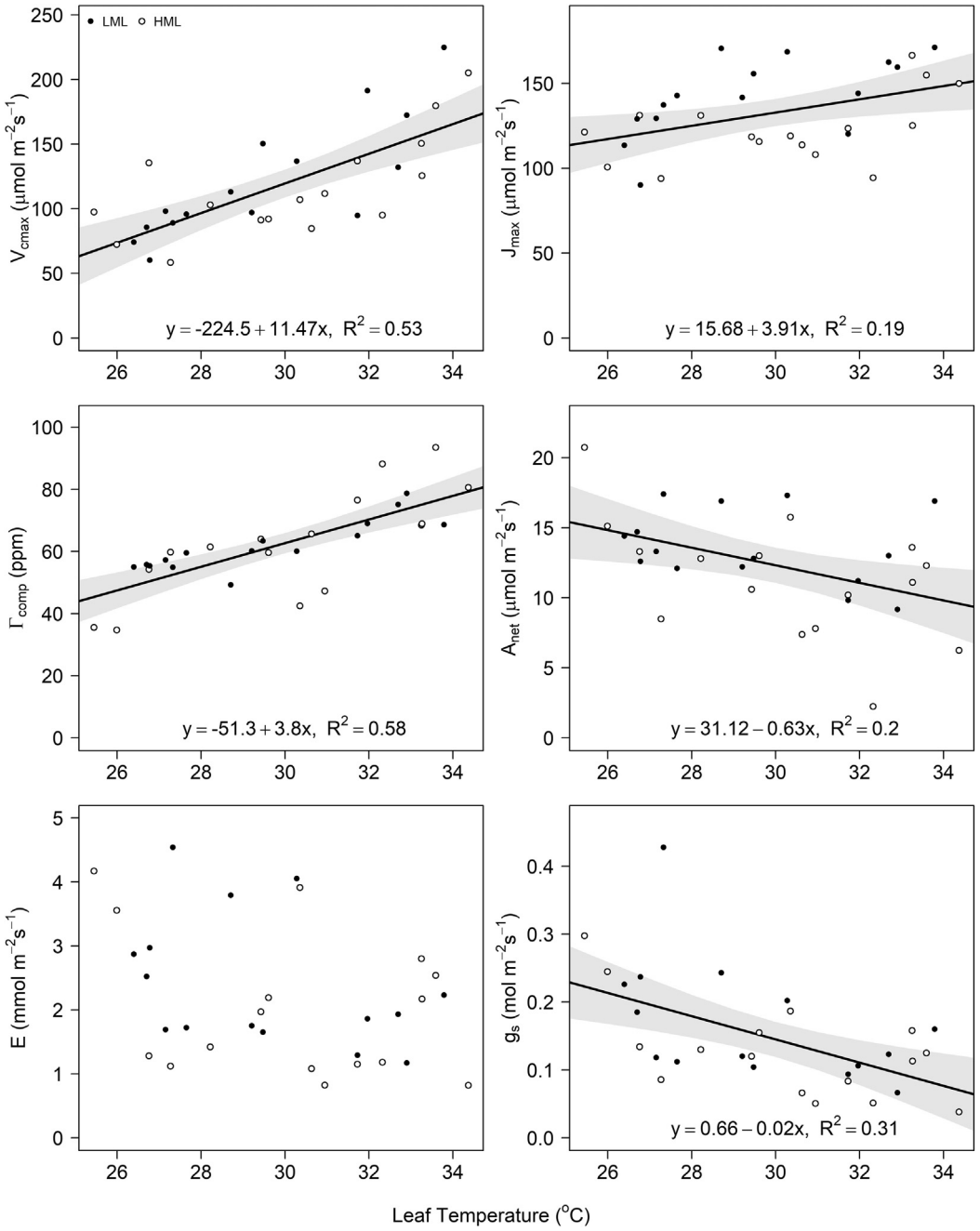

Fig. 5. Response of photosynthesis parameters to leaf temperature in high (HML) and low (LML) metal load trees. Solid line represents the linear regression of pooled LML and HML data. Gray band represents 95% confidence interval around the regression line.

11 to 88 g m^{-2}), suggesting that all LSP trees may be producing lower LMA leaves in response to trace metal exposure. Given that lower LMA is associated with shorter leaf lifespan (Wright et al., 2004), the lower LMA in the high metal load group, in particular, may lead to higher rates of leaf turnover. The aforementioned processes would divert carbon from accumulating as wood, which is consistent with the reduction in basal growth rates previously observed in trees from high metal load plots at the site (Gallagher et al., 2008a).

The effects of contrasting soil metal concentrations on the photosynthetic parameters of *B. populifolia* were not as drastic as initially hypothesized. While intermittent, the decline in R_{dark} in the high metal load group may suggest that these trees allocated less energy to protection mechanisms against metal contamination (Losch, 2004; Romanowska et al., 2002; Vassilev et al., 1997). Similar results were observed by Hermle et al. (2007) for *Salix viminalis* L. and *Populus tremula* L. grown in soil contaminated with smelter dust. However, given the marginally lower rates of R_{dark} observed in the leaves from high metal load plots, it is not clear that these *B. populifolia* leaves mounted a strong protection response. The decrease in R_{dark} may alternatively be attributable to the concurrently depressed rates of A_{max} and A_{net}; with less carbohydrate produced, less substrate is available for respiration (Cannell and Thornley, 2000).

An increase in Γ_{comp} was observed in the high metal load trees during some months, which can indicate an increase in photorespiration, i.e., the release of CO_2 during photosynthesis when O_2 binds to RuBP rather than CO_2 (Di Baccio et al., 2009). Photorespiration can increase

as stomatal closure limits CO_2 supply, though it can also increase to negate the effects of other stresses (Wingler et al., 2000). High metal load trees' g_s rates were lower than those in the low metal load group, an effect which also manifested as elevated iWUE in the high metal load trees. This reduction in g_s makes it difficult to determine whether the increase in Γ_{comp} is a direct result of stomatal limitation or is a stress response to elevated trace metal concentrations in the leaves themselves.

Numerous laboratory and greenhouse studies have demonstrated that photosynthesis and related gas exchange parameters are frequently diminished with increasing exposure to a variety of heavy metals (Di Baccio et al., 2009; Gaudet et al., 2011; Pereira et al., 2016; Santana et al., 2012). However, differences in methodologies and reporting make it extremely difficult to compare soil trace metal concentrations across studies. Consequently, it is possible that the gradient of trace metal concentrations in our plots was not as wide as those assessed in other studies, which may account for the smaller differences observed in this study. That said, while laboratory and greenhouse based approaches are valuable for elucidating mechanistic responses, they do not reflect complex field conditions where multiple, interacting factors mediate the leaf-level response to elevated trace metals, including community level interactions (Krumins et al., 2015) and plant-mycorrhyzal associations (Yang et al., 2015). Additionally, as suggested by Radwanski et al. (2017), photosynthesis in LSP trees may be robust across the TML gradient because the site was self-seeded and trace metal contamination likely acted as an abiotic filter, in this case favoring the establishment of genotypes with high tolerance to elevated trace metal concentrations.

4.2. Temperature and drought response

That iWUE was reduced in the high metal load group immediately after the July 2015 heat wave suggests that these trees were more strongly affected by the heat wave, supporting our initial hypothesis. Prior studies of the interacting effects of trace metals and water stress on plant growth have yielded mixed results. In a containerized experiment, the dry mass of *B. papyrifera* seedlings exposed to high concentrations of Cu and Ni were less affected by drought than control seedlings (Santala and Ryser, 2009). The authors posited that, because the seedlings were already impaired by metal exposure, they had a lower water demand and were consequently less prone to drought stress. However, the combination of drought and heavy metal stress has also been observed to reduce growth additively (de Silva et al., 2012).

For leaf temperatures spanning 25 to 35 °C, trace element contamination did not alter the relationship between leaf temperature and leaf gas exchange parameters, contrary to our hypothesis. Given that other studies have observed greater thermotolerance in plants exposed to heavy metals (Howarth, 1990), it is possible that the indistinguishable temperature responses between LML and HML trees resulted from such a protection mechanism. However, further research would be needed to confirm this hypothesis. Within the temperature range of our study, it is possible that leaves were either not exposed to heat for a sufficient duration to induce heat shock or that still-higher temperatures were needed to induce non-stomatal responses.

5. Conclusions

To further our understanding of the effects of soil pollution on primary productivity in early successional hardwood forests, we measured leaf level gas exchange parameters of mature *Betula populifolia* trees growing in contrasting trace metal contamination levels. The results of this two year study suggest that the photosynthetic rates and related biophysical parameters of this population are fairly robust across the pollution gradient. When photosynthesis differed by total metal load, the effects were transient, demonstrating the importance of field studies to capture temporally-varying effects. That there were differences in leaf mass per area between trees in soils with low vs. high metal loads underscores the fact that trace metal contamination can impact resource allocation in addition to physiology. Moreover, the heat wave in July 2015 did reduce water use efficiency in high metal load trees, suggesting that *B. populifolia* exposed to high soil metal concentrations may be more susceptible to climatic stress. Anthropogenic soils can create novel ecosystems that may function differently from more commonly studied ecosystems. Consequently, expectations for their functionality and resilience should be adapted to fit these unique conditions rather than being based on assumptions from traditional plant assemblages.

Funding

This work was supported by two McIntire-Stennis Capacity Grants (numbers 17325 and 17350) from the United States Department of Agriculture's National Institute of Food and Agriculture.

Acknowledgements

Special thanks to Karina Schaffer for input on the study design and equipment loans, as well as to the students who assisted with field work: Isabella Cocuzza, Catherine Dillon, Booker George, Longjun Ju, and Han Yan. We are also grateful to the New Jersey Department of Environmental Protection Division of Parks and Forestry for their continued support of research at Liberty State Park.

Appendix A. Methods of soil analysis

To characterize soil physical and chemical properties of the four study plots (Table 1), 3 to 4 samples were collected with a slide corer from the top 15 cm of soil (excluding leaf litter) from random locations within each plot. The <2 mm fraction of soil was analyzed for pH, soil texture, total carbon and nitrogen, as well as selected macronutrients. Analyses were conducted by the New Jersey Agricultural Experiment Station Soil Testing Lab (New Brunswick, USA). pH was measured in a slurry with a 1:1 ratio by volume of soil to water with a dS975 SevenExcellence Multiparameter pH meter (Mettler Toledo, Columbus, OHUSA). Soil texture was determined using the hydrometer method from a 50 g sample (<2 mm) dispersed with 50 mL of 10% sodium hexametaphosphate. Free ammonia and total Kjeldahl nitrogen (TKN) were determined using an AutoAnalyzer III (wavelength = 667 nm, Bran + Luebbe Analytics, Norderstedt, Germany) following EPA Method 351.1. A Mehlich-3 extractant was used to determine plant available P, K, Mg, and Ca with an iCAP 7000 inductively coupled plasma optical emission spectrophotometer (Themo Scientific, Waltham, USAMA). Note that the Mehlich-3 extractions approximate plant available element concentrations rather than total or pseudo-total concentrations (Mehlich, 1984). Total carbon (TC) and total nitrogen (TN) were determined from 350 (±50 mg) samples using a dry combustion method at 900 °C with a vario MAX cube C/N analyzer (Elementar Americas, Mt. Laurel, NJ, USA) and helium as a carrier gas. The upper horizons of Liberty State Park soils have a high coal dust and fragment content (Soil Survey Staff, 2010), which would have inflated traditional loss on ignition (LOI) measurements made at a lower temperature by combusting some, but not all, of the coal carbon (Rawlins et al. 2008). Instead, we conducted an analysis of the total carbon, which completely measures both recent litter-derived soil organic carbon and coal carbon (Ussiri and Lal, 2008). To help discern the effects of recent vs. geogenic soil organic carbon, measurements of total nitrogen (TN) were included, presuming that TN would represent recent soil organic matter reasonably well.

Appendix B. Temperature correction factors

Table B.1
Values used to adjust V_{cmax} and J_{max} to 25 °C. ΔH_a is the activation energy and c is a scaling constant. The scaling constants for V_{cmax} and J_{max} were normalized so the parameters equal 1 at 25 °C . K_c, Michaelis-Menten constant of Rubisco for CO_2; K_O, Michaelis-Menten constant of Rubisco for O_2; Γ*, Photorespiratory compensation point.

	Parameter at 25 °C	c (−)	ΔH_a (kJ mol^{-1})
K_C (μmol CO_2 mol air)[a]	404.9	38.05	79.43
K_O (μmol O_2 mol air)[a]	278.4	20.30	36.38
Γ* (μmol CO_2 mol air)[a]	42.75	19.02	37.83
V_{cmax} (μmol CO_2 m^{-2} s^{-1})[a]	1.00	26.35	65.33
J_{max} (μmol e^- m^{-2} s^{-1})[b]	1.00	17.70	43.90

[a] Bernacchi et al., 2001.
[b] Bernacchi et al., 2003.

Appendix C. Metal load and month-year group means

Table C.1
Least-squares means (± 1 SE) for photosynthesis parameters under low (LML) and high (HML) metal loads by month in 2014. . † indicates data were log transformed.

Month	Metal load	V_{cmax}(μmol m^{-2} s^{-1})	J_{max} (μmol m^{-2} s^{-1})†	Γ_{comp} (ppm^{-})†	A_{max} (μmol m^{-2} s^{-1})	φ (μmol CO_2 μmol^{-1} photon)	I_{comp} (μmol m^{-2} s^{-1})†	R_{dark} (μmol m^{-2} s^{-1})	A_{net} (μmol m^{-2} s^{-1})	E (mmol m^{-2} s^{-1})†	g_s (mol m^{-2} s^{-1})†	iWUE (μmol CO_2 mol^{-1} H_2O)
2014												
May	LML	51.7 ± 4.2	4.53 ± 0.09	4 ± 0.07	8.4 ± 1.1	0.062 ± 0.004	2.96 ± 0.13	1.2 ± 0.1	8.9 ± 1.1	0.41 ± 0.22	−2.13 ± 0.24	68.7 ± 9.1
	HML	60.8 ± 4.2	4.77 ± 0.07	3.95 ± 0.07	7.9 ± 1.1	0.071 ± 0.004	2.74 ± 0.13	1.1 ± 0.1	8.4 ± 1.1	0.44 ± 0.22	−2.21 ± 0.24	73.7 ± 9.2
Jun	LML	52.5 ± 4.4	4.67 ± 0.1	4 ± 0.07	9.8 ± 1.2	0.066 ± 0.004	2.6 ± 0.13	1 ± 0.1	11.2 ± 1.1	0.67 ± 0.22	−1.73 ± 0.25	56.7 ± 9.6
	HML	55 ± 4.2	4.65 ± 0.08	4.01 ± 0.07	8.3 ± 1.1	0.067 ± 0.004	2.78 ± 0.13	1.1 ± 0.1	8.8 ± 1.1	0.35 ± 0.22	−2.23 ± 0.24	76 ± 9.2
Jul	LML	64 ± 4.2	4.79 ± 0.08	4.01 ± 0.07	8.6 ± 1.1	0.069 ± 0.004	2.67 ± 0.13	0.9 ± 0.1	9 ± 1.1	0.38 ± 0.22	−2.46 ± 0.24	87.1 ± 9.1
	HML	53.2 ± 4.2	4.52 ± 0.07	4.05 ± 0.07	7.5 ± 1.1	0.055 ± 0.004	2.35 ± 0.13	0.6 ± 0.1	8 ± 1.1	0.35 ± 0.22	−2.64 ± 0.24	106.3 ± 9.2
Aug	LML	51.1 ± 4.2	4.86 ± 0.12	4.21 ± 0.07	4.9 ± 1.2	0.078 ± 0.004	2.78 ± 0.13	1.1 ± 0.1	5 ± 1.1	−0.1 ± 0.22	−3.16 ± 0.24	104.9 ± 9.1
	HML	59.8 ± 4.2	4.67 ± 0.09	4.14 ± 0.07	7.4 ± 1.1	0.069 ± 0.004	2.67 ± 0.13	1 ± 0.1	7.8 ± 1.1	0.1 ± 0.22	−2.83 ± 0.24	113.7 ± 9.2
Sep	LML	43.8 ± 4.2		4.2 ± 0.07	4.6 ± 1.1	0.072 ± 0.004	2.39 ± 0.13	0.7 ± 0.1	4.9 ± 1.1	−0.27 ± 0.22	−3.3 ± 0.24	122.7 ± 9.1
	HML	40 ± 4.2		4.35 ± 0.07	3.5 ± 1.1	0.063 ± 0.004	2.74 ± 0.13	0.9 ± 0.1	3.8 ± 1.1	−0.31 ± 0.22	−3.35 ± 0.24	100.7 ± 9.2

Table C.2
Least-squares means (± 1 SE) for photosynthesis parameters under low (LML) and high (HML) metal loads by month in 2015. † indicates data were log transformed.

Month	Metal load	V_{cmax} (μmol m^{-2} s^{-1})	J_{max} (μmol m^{-2} s^{-1})†	Γ_{comp} (μmol CO_2 mol^{-1} air)†	A_{max} (μmol m^{-2} s^{-1})	φ (μmol CO_2 μmol^{-1} photon)	I_{comp} (μmol m^{-2} s^{-1})†	R_{dark} (μmol m^{-2} s^{-1})	A_{net} (μmol m^{-2} s^{-1})	E (mmol m^{-2} s^{-1})	g_s (mol m^{-2} s^{-1})†	iWUE (μmol CO_2 mol^{-1} H_2O)	LMA (g m^{-2})
2015													
May	LML	73.6 ± 5.4	4.7 ± 0.1	4.3 ± 0.09	9.9 ± 1.2	0.061 ± 0.004	2.73 ± 0.13	1 ± 0.1	9.8 ± 1.1	0.5 ± 0.22	−2.38 ± 0.24	94 ± 9.1	50.5 ± 2.1
	HML	63.3 ± 4.2	4.59 ± 0.08	4.32 ± 0.07	7.2 ± 1.1	0.056 ± 0.004	2.79 ± 0.13	0.9 ± 0.1	7.5 ± 1.1	0.26 ± 0.22	−2.84 ± 0.24	105.8 ± 9.2	50.6 ± 2.2
Jun	LML	60.8 ± 4.4	4.69 ± 0.09	4.56 ± 0.07	9 ± 1.1	0.062 ± 0.004	2.91 ± 0.13	1.1 ± 0.1	9.4 ± 1.1	0.64 ± 0.22	−2.17 ± 0.24	85.6 ± 9.1	53.5 ± 2.1
	HML	68.9 ± 4.2	4.59 ± 0.08	4.3 ± 0.07	7.2 ± 1.2	0.058 ± 0.005	2.55 ± 0.14	0.8 ± 0.1	7.5 ± 1.1	0.49 ± 0.22	−2.62 ± 0.24	91.2 ± 9.2	43.5 ± 2.1
Jul	LML	28.6 ± 7.7		4.91 ± 0.12	1.7 ± 1.7	0.052 ± 0.006	2.57 ± 0.2	0.6 ± 0.2	1.8 ± 1.2	−2.07 ± 0.24	−4.59 ± 0.28	136.2 ± 11.6	51.8 ± 2.1
	HML	32.6 ± 4.4		4.67 ± 0.07	1.4 ± 1.3	0.048 ± 0.005	2.6 ± 0.15	0.5 ± 0.1	1.9 ± 1.2	−1.72 ± 0.22	−4.66 ± 0.25	99.9 ± 10.2	44.2 ± 2.2
Aug	LML				4 ± 1.2	0.058 ± 0.004	2.83 ± 0.13	0.8 ± 0.1	4.5 ± 1.1	−0.57 ± 0.22	−3.25 ± 0.24	76.9 ± 9.1	54.2 ± 2.1
	HML				3.7 ± 1.3	0.061 ± 0.005	2.57 ± 0.15	0.7 ± 0.1	4.5 ± 1.1	−0.82 ± 0.22	−3.4 ± 0.24	83 ± 9.2	51.2 ± 2.1
Sep	LML								4.6 ± 1.1	−0.51 ± 0.22	−3.02 ± 0.24	91.5 ± 9.1	52.2 ± 2.1
	HML								5.7 ± 1.1	−0.09 ± 0.22	−2.64 ± 0.24	79 ± 9.2	46.6 ± 2.1

Appendix D. Stomatal conductance relationship to C_i/C_a

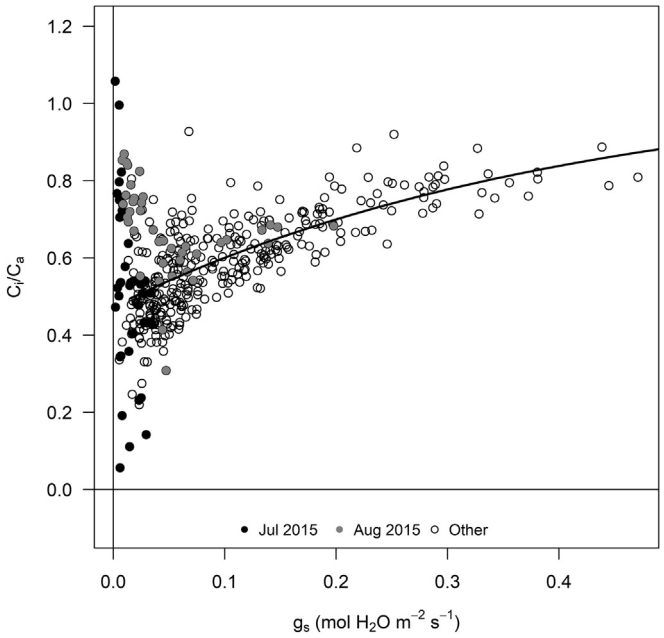

Fig. D.1. Relationship between stomatal conductance (g_s) and the ratio of intercellular CO_2 to ambient CO_2 (C_i/C_a). Solid line depicts function for an exponential rise to maximum (Singh and Reddy, 2011) for all data (high and low metal load). Filled circles depict measurements made in July 2015 immediately after the heat wave; gray circles depict measurements made the following month (August 2015); open circles depict all other measurements. The curve was fit using data where $g_s > 0.01$ mol H_2O m^{-2} s^{-1} (based on minimum C_i/C_a): $C_i/C_a = 0.47 + 0.58*(1\text{-}e^{(-2.45*gs)})$.

References

Ajmone-Marsan, F., Biasioli, M., 2010. Trace elements in soils of urban areas. Water Air Soil Pollut. 213 (1–4), 121–143.

Allen, R.G., Pereira, L.S., Raes, D., Smith, M., 1998. Crop Evapotranspiration - Guidelines for Computing Crop Water Requirements. FAO Irrigation and Drainage Paper 56. Rome, Italy.

Al-Tabbaa, A., Smith, S., De Munck, C., Dixon, T., Doak, J., Garvin, S., Raco, M., 2007. Climate change, pollutant linkage and Brownfield Regeneration. In: Dixon, T., Raco, M., Catney, P., Lerner, D. (Eds.), Sustainable Brownfield Regeneration. Blackwell Publishing, Oxford, UK.

André, O., Vollenweider, P., Günthardt-Goerg, M.S., 2006. Foliage response to heavy metal contamination in Sycamore Maple (*Acer pseudoplatanus* L.). For. Snow Landsc. Res 80 (3), 275–288.

Bates, D., Machler, M., Bolker, B., Walker, S., 2015. Fitting linear mixed-effects models using lme4. J. Stat. Softw. 67 (1), 1–48.

Bernacchi, C.J., Singsaas, E.L., Pimentel, C., A.R. Jr, Portis, Long, S.P., 2001. Improved temperature response functions for models of Rubisco-limited photosynthesis. Plant Cell Environ. 24 (2), 253–260.

Bernacchi, C.J., Pimentel, C., Long, S.P., 2003. *In vivo* temperature response functions of parameters required to model RuBP-limited photosynthesis. Plant Cell Environ. 26 (9), 1419–1430.

Bleeker, P.M., Assunção, A.G.L., Teiga, P.M., De Koe, T., Verkleij, J.A.C., 2002. Revegetation of the acidic, As contaminated Jales mine spoil tips using a combination of spoil amendments and tolerant grasses. Sci. Total Environ. 300 (1–3), 1–13.

Boone, R., Tardif, J., Westwood, R., 2004. Radial growth of oak and aspen near a coal-fired station, Manitoba, Canada. Tree-Ring Research 60 (1), 45–58.

Borgegard, S.-O., Rydin, H., 1989. Biomass, root penetration and heavy metal uptake in birch in a soil cover over copper tailings. J. Appl. Ecol. 26, 585–595.

Brodribb, T., 1996. Dynamics of changing intercellular CO_2 concentration (c_i) during drought and determination of minimum functional c_i. Plant Physiol. 111 (1), 179–185.

Cannell, M.G.R., Thornley, J.N.M., 2000. Modelling the components of plant respiration: some guiding principles. Ann. Bot. 85, 45–54.

Chen, A., Lichstein, J.W., Osnas, J.L.D., Pacala, S.W., 2014. Species-independent down-regulation of leaf photosynthesis and respiration in response to shading: evidence from six temperate tree species. PLoS ONE 9 (4), e91798.

Dahle, G.A., Gallagher, F.J., Gershensond, D., Schäfer, K.V.R., Grabosky, J.C., 2014. Allometric and mass relationships of *Betula populifolia* in a naturally assembled urban brownfield: implications for carbon modeling. Urban Ecosystems 17 (4), 1147–1160.

De Laender, F., De Schamphelaere, K.A.C., Vanrolleghem, P.A., Janssen, C.R., 2008. Validation of an ecosystem modelling approach as a tool for ecological effect assessments. Chemosphere 71 (3), 529–545.

de Mendiburu F., Agricolae: Statistical Procedures for Agricultural Research, R package version 1.2

de Silva, N.D.G., Cholewa, E., Ryser, P., 2012. Effects of combined drought and heavy metal stresses on xylem structure and hydraulic conductivity in red maple (*Acer rubrum* L.). J. Exp. Bot. 63 (16), 5957–5966.

Di Baccio, D., Tognetti, R., Minnocci, A., Sebastiani, L., 2009. Responses of the *Populus* × *euramericana* clone I-214 to excess zinc: carbon assimilation, structural modifications, metal distribution and cellular localization. Environ. Exp. Bot. 67 (1), 153–163.

Doick, K.J., Sellers, G., Castan-Broto, V., Silverthorne, T., 2009. Understanding success in the context of brownfield greening projects: the requirement for outcome evaluation in urban greenspace success assessment. Urban For. Urban Green. 8 (3), 163–178.

Duursma, R.A., 2015. Plantecophys - an R package for analysing and modelling leaf gas exchange data. PLoS ONE 10 (11), e0143346.

Farquhar, G.D., von Caemmerer, S., Berry, J.A., 1980. A biochemical model of photosynthetic CO_2 assimilation in leaves of C_3 species. Planta 90, 78–90.

Ferreira, T., Rasband, W.S., 2012. ImageJ User Guide - IJ 1.46. U.S. National Institutes of Health, Bethesda, MD.

Forbes, V.E., Calow, P., 2013. Developing predictive systems models to address complexity and relevance for ecological risk assessment. Integr. Environ. Assess. Manag. 9 (3), e75–80.

Fox, J., Weisberg, S., 2011. An R Companion to Applied Regression. 2nd edition. Sage, Thousand Oaks, CA.

French, C.J., Dickinson, N.M., Putwain, P.D., 2006. Woody biomass phytoremediation of contaminated brownfield land. Environ. Pollut. 141 (3), 387–395.

Frouz, J., Prach, K., Pižl, V., Háněl, L., Starý, J., Tajovský, K., Materna, J., Balík, V., Kalčík, J., Řehounková, K., 2008. Interactions between soil development, vegetation and soil fauna during spontaneous succession in post mining sites. Eur. J. Soil Biol. 44 (1), 109–121.

Gallagher, F.J., Pechmann, I., Bogden, J.D., Grabosky, J., Weis, P., 2008a. Soil metal concentrations and productivity of *Betula populifolia* (gray birch) as measured by field spectrometry and incremental annual growth in an abandoned urban Brownfield in New Jersey. Environ. Pollut. 156 (3), 699–706.

Gallagher, F.J., Pechmann, I., Bogden, J.D., Grabosky, J., Weis, P., 2008b. Soil metal concentrations and vegetative assemblage structure in an urban brownfield. Environ. Pollut. 153 (2), 351–361.

Gallagher, F.J., Pechmann, I., Holzapfel, C., Grabosky, J., 2011. Altered vegetative assemblage trajectories within an urban brownfield. Environ. Pollut. 159 (5), 1159–1166.

Gallagher, F.J., Caplan, J.S., Krumins, J.A., Grabosky, J.C., 2015. Root growth responses to soil amendment in an urban brownfield. Ecol. Restor. 33 (1), 10–13.

Gaudet, M., Pietrini, F., Beritognolo, I., Iori, V., Zacchini, M., Massacci, A., Mugnozza, G.S., Sabatti, M., 2011. Intraspecific variation of physiological and molecular response to cadmium stress in *Populus nigra* L. Tree Physiol. 31 (12), 1309–1318.

Hermle, S., Günthardt-Goerg, M.S., Schulin, R., 2006. Effects of metal-contaminated soil on the performance of young trees growing in model ecosystems under field conditions. Environ. Pollut. 144 (2), 703–714.

Hermle, S., Vollenweider, P., Günthardt-Goerg, M.S., McQuattie, C.J., Matyssek, R., 2007. Leaf responsiveness of *Populus tremula* and *Salix viminalis* to soil contaminated with heavy metals and acidic rainwater. Tree Physiol. 27 (11), 1517–1531.

Hooper, M.J., Glomb, S.J., Harper, D.D., Hoelzle, T.B., Mcintosh, L.M., Mulligan, D.R., 2016. Integrated risk and recovery monitoring of ecosystem restorations on contaminated sites. Integr. Environ. Assess. Manag. 12 (2), 284–295.

Howarth, C.J., 1990. Heat shock proteins in sorghum and pearl millet; ethanol, sodium arsenite, sodium malonate and the development of thermotolerance. J. Exp. Bot. 41 (7), 877–883.

Joesting, H.M., McCarthy, B.C., Brown, K.J., 2009. Determining the shade tolerance of American chestnut using morphological and physiological leaf parameters. For. Ecol. Manag. 257 (1), 280–286.

Krumins, J.A., Goodey, N.M., Gallagher, F., 2015. Plant–soil interactions in metal contaminated soils. Soil Biol. Biochem. 80, 224–231.

Kubiske, M.E., Pregitzer, K.S., 1996. Effects of elevated CO_2 and light availability on the photosynthetic light response of trees of contrasting shade tolerance. Tree Physiol. 16 (3), 351–358.

Larson, C., 2014. China gets serious about its pollutant-laden soil. Science 343 (6178), 1415–1416.

Lenth, R., 2016. Least-squares means: the R package lsmeans. J. Stat. Softw. 69 (1), 1–33.

Losch, R., 2004. Plant mitochondrial respiration under the influence of heavy metals. In: Prasad, M.N.V. (Ed.), Heavy Metal Stress in Plants: From Biomolecules to Ecosystems. Springer, Berlin, pp. 182–200.

Maggio, A., Joly, R.J., 1995. Effects of mercuric chloride on the hydraulic conductivity of tomato root systems. Plant Physiol. 109, 331–335.

Martin, B.T., Jager, T., Nisbet, R.M., Preuss, T.G., Hammers-Wirtz, M., Grimm, V., 2013. Extrapolating ecotoxicological effects from individuals to populations: a generic approach based on dynamic energy budget theory and individual-based modeling. Ecotoxicology 22 (3), 574–583.

Martin, B., Jager, T., Nisbet, R., 2014. Limitations of extrapolating toxic effects on reproduction to the population level. Ecol. Appl. 24 (8), 1972–1983.

Medvigy, D., Wofsy, S.C., Munger, J.W., Hollinger, D.Y., Moorcroft, P.R., 2009. Mechanistic scaling of ecosystem function and dynamics in space and time: Ecosystem Demography model version 2. J. Geophys. Res. 114 (G1), G01002.

Mehlich, A., 1984. Mehlich 3 soil test extractant: a modification of the Mehlich 2 extractant. Commun. Soil Sci. Plant Anal. 15 (2), 1409–1416.

Moustakas, M., Ouzounidou, G., Symeonidis, L., Karataglis, S., 1997. Field study of the effects of excess copper on wheat photosynthesis and productivity. Soil Sci. Plant Nutr. 43 (3), 531–539.

Murray, P., Ge, Y., Hendershot, W.H., 2000. Evaluating three trace metal contaminated sites: a field and laboratory investigation. Environ. Pollut. 107 (1), 127–135.

Mysliwa-Kurdziel, B., Prasad, M.N.V., Strzalka, K., 2004. Photosynthesis in heavy metal stressed plants. In: Prasad, M.N.V. (Ed.), Heavy Metal Stress in Plants: From Biomolecules to Ecosystems. Springer, Berlin, pp. 146–181.

New Jersey Weather, Climate Network, 2016. Data Viewer - Jersey City Station 3411. Office of the New Jersey State Climatologist http://www.njweather.org/data accessed Oct. 11, 2016.

Panagos, P., Van Liederkerke, M., Yigini, Y., Montanarella, L., 2013. Contaminated sites in Europe: review of the current situation based on data collected through a European network. J. Environ. Public Health 2013 (2013), 158764.

Pavao-Zuckerman, M.A., 2008. The nature of urban soils and their role in ecological restoration in cities. Restor. Ecol. 16 (4), 642–649.

Pereira, M.P., Rodrigues, L.C., Corrêa, F.F., de Castro, E.M., Ribeiro, V.E., Pereira, F.J., 2016. Cadmium tolerance in *Schinus molle* trees is modulated by enhanced leaf anatomy and photosynthesis. Trees - Structure and Function 30 (3), 807–814.

Poschenrieder, C., Barcelo, J., 2004. Water relations in heavy metal stressed plants. In: Prasad, M.N.V. (Ed.), Heavy Metal Stress in Plants: From Biomolecules to Ecosystems. Springer, Berlin, pp. 223–248.

Prach, K., Pyšek, P., 2001. Using spontaneous succession for restoration of human-disturbed habitats: experience from Central Europe. Ecol. Eng. 17 (1), 55–62.

Prioul, J.L., Chartier, P., 1977. Partitioning of transfer and carboxylation components of intracellular resistance to photosynthetic CO_2 fixation: a critical analysis of the methods used. Ann. Bot. 41 (4), 789–800.

R Development Core Team, 2016. R: A Language and Environment for Statistical Computing. R Foundation for Statistical Computing, Vienna, Austria.

Rachmilevitch, S., DaCosta, M., Huang, B., 2006. Physiological and biochemical indicators for stress tolerance. In: Huang, B. (Ed.), Plant-Environment Interactions. CRC Press, Boca Raton, Florida, pp. 321–356.

Radwanski, D., Vanderklein, D.W., Schäfer, K.V.R., 2017. Physiology and carbon allocation of two co-occurring poplar species in an urban brownfield. Environ. Pollut. 223, 497–506.

Rawlins, B.G., Vane, C.H., Kim, A.W., Tye, A.M., Kemp, S.J., Bellamy, P.H., 2008. Methods for estimating types of soil organic carbon and their application to surveys of UK urban areas. Soil Use Manag. 24 (1), 47–59.

Reich, P.B., Ellsworth, D.S., Uhl, C., 1995. Leaf carbon and nutrient assimilation and conservation in species of differing successional status in an oligotrophic Amazonian forest. Funct. Ecol. 9 (1), 65–76.

Renninger, H.J., Wadhwa, S., Gallagher, F.J., Vanderklein, D., Schäfer, K.V.R., 2013. Allometry and photosynthetic capacity of poplar (*Populus deltoides*) along a metal contamination gradient in an urban brownfield. Urban Ecosystems 16 (2), 247–263.

Robb, J., Busch, L., Rauser, W.E., 1980. Zinc toxicity and xylem vessel wall alteration in white beans. Ann. Bot. 46 (1), 43–50.

Robinson, B.H., Bañuelos, G., Conesa, H.M., Evangelou, M.W.H., Schulin, R., 2009. The phytomanagement of trace elements in soil. Crit. Rev. Plant Sci. 28 (4), 240–266.

Rohr, J.R., Salice, C.J., Nisbet, R.M., Rohr, J.R., Salice, C.J., Nisbet, R.M., 2016. The pros and cons of ecological risk assessment based on data from different levels of biological organization. Crit. Rev. Toxicol. 46 (9), 756–784.

Romanowska, E., Igamberdiev, A.U., Parys, E., Gardeström, P., 2002. Stimulation of respiration by Pb^{2+} in detached leaves and mitochondria of C_3 and C_4 plants. Physiol. Plant. 116, 148–154.

Romero Lankao, P., Davidson, D.J., Diffenbaugh, N.S., Kinney, P.L., Kirshen, P., Kovacs, P., Ruiz, L.V., 2014. North America. In: Barros, V.R., Field, C.B., Dokken, D.J., Mastrandrea, M.D., Mach, K.J., Bilir, T.E., Chatterjee, M., Ebi, K.L., Estrada, Y.O., Genova, R.C., Girma, B., Kissel, E.S., Levy, A.N., MacCracken, S., Mastrandrea, P.R., White, L.L. (Eds.), Climate Change 2014: Impacts, Adaptation, and Vulnerability. Part B: Regional Aspects. Cambridge University Press, Cambridge, UK and New York, NY, USA, pp. 1439–1498.

Santala, K.R., Ryser, P., 2009. Influence of heavy-metal contamination on plant response to water availability in white birch, *Betula papyrifera*. Environ. Exp. Bot. 66 (2), 334–340.

Santana, K.B., de Almeida, A.A.F., Souza, V.L., Mangabeira, P.A.O., da C. Silva, D., Gomes, F.P., Dutruch, L., Loguercio, L.L., 2012. Physiological analyses of *Genipa americana* L. reveals a tree with ability as phytostabilizer and rhizofilterer of chromium ions for phytoremediation of polluted watersheds. Environ. Exp. Bot. 80, 35–42.

Sarkar, D., 2008. Lattice: Multivariate Data Visualization with R. Springer, New York.

Searle, S.R., Speed, F.M., Milliken, G.A., 1980. Population marginal means in the linear model: an alternative to least squares means. Am. Stat. 34 (4), 216–221.

Sebelikova, L., Rehounkova, K., Prach, K., 2016. Spontaneous revegetation vs. forestry reclamation in post-mining sand pits. Environ. Sci. Pollut. Res. 23 (14), 13598–13605.

Sharkey, T.D., Bernacchi, C.J., Farquhar, G.D., Singsaas, E.L., 2007. Fitting photosynthetic carbon dioxide response curves for C_3 leaves. Plant Cell Environ. 30 (9), 1035–1040.

Shi, G., Cai, Q., 2009. Leaf plasticity in peanut (*Arachis hypogaea* L.) in response to heavy metal stress. Environ. Exp. Bot. 67 (1), 112–117.

Singh, S.K., Reddy, K.R., 2011. Regulation of photosynthesis, fluorescence, stomatal conductance and water-use efficiency of cowpea (*Vigna unguiculata* [L.] Walp.) under drought. J. Photochem. Photobiol. B Biol. 105 (1), 40–50.

Soil Survey Staff, 2010. Ladyliberty Soil Series: Primary Characterization Data.

United Nations, 2015. World Urbanization Prospects: The 2014 Revision (New York City).

Ussiri, D.A.N., Lal, R., 2008. Method for Determining Coal Carbon in the Reclaimed Minesoils Contaminated with Coal. Soil Sci. Soc. Am. J. 72 (1), 231.

Vassilev, A., Yordanov, I., Tsonev, T., 1997. Effects of Cd^{2+} on the physiological state and photosynthetic activity of young barley plants. Photosynthetica 34 (2), 293–302.

Wayne, P.M., Bazzaz, F.A., 1993. Birch seedling responses to daily time courses of light in experimental forest gaps and shadehouses. Ecology 74 (5), 1500–1515.

Wingler, A., Lea, P.J., Quick, W.P., Leegood, R.C., 2000. Photorespiration: metabolic pathways and their role in stress protection. Philos. Trans. R. Soc. Lond. Ser. B Biol. Sci. 355 (1402), 1517–1529.

Wright, I.J., Reich, P.B., Westoby, M., Ackerly, D.D., Baruch, Z., Bongers, F., Cavender-Bares, J., Chapin, T., Cornelissen, J.H.C., Diemer, M., Flexas, J., Garnier, E., Groom, P.K., Gulias, J., 2004. The worldwide leaf economics spectrum. Nature 428, 821–827.

Yang, Y., Han, X., Liang, Y., Ghosh, A., Chen, J., Tang, M., 2015. The combined effects of arbuscular mycorrhizal fungi (AMF) and lead (Pb) stress on Pb accumulation, plant growth parameters, photosynthesis, and antioxidant enzymes in *Robinia pseudoacacia* L. PLoS ONE 10 (12), e0145726.